JOURNAL OF MATERIALS SCIENCE 14 (1979) 2625–2636

Recovery of a creep-deformed Type 316 stainless steel

D. G. MORRIS*, D. R. HARRIES
Metallurgy Division, AERE, Harwell, Oxon, UK

The recovery of the dislocation structures produced in a Type 316 steel during creep has been examined by annealing over a range of temperatures and times, both in the presence and in the absence of stress. The influence of dislocation recovery on subsequent reloading behaviour has also been examined.

Initial dislocation recovery occurs rapidly but the rate of recovery subsequently decreases as precipitate effects become more important. Dislocation recovery in the early, rapid stage appears to be controlled by vacancy diffusion between the dislocation links. The application of stress during recovery leads to an enhancement of the recovery rate in agreement with the network coarsening model whilst the incremental strains observed on reloading after recovery correlate well with the changes in dislocation structure produced during the recovery periods.

1. Introduction

The recovery of dislocation structures during elevated temperature annealing has previously been considered in terms of coarsening of the network structure as a result of dislocation climb [1–5]. Climb, by jog movement on dislocations, depends either on the rate of vacancy emission from jogs or on vacancy diffusion through the lattice [6] and the recovery rate (dl/dt) may be expressed (see Appendix I for list of symbols) as [6, 7]:

$$\frac{dl}{dt} = \frac{2D_s b C_j}{kT} \frac{\tau}{l} \quad (1)$$

or

$$\frac{dl}{dt} = \frac{2D_s b}{kT \ln (l/b)} \frac{\tau}{l} \quad (2)$$

Other expressions have been derived to describe the recovery process, the most notable being those of Weertman [8] which consider the effects of dislocation pile-ups on recovery; such mechanisms are unlikely to be important in the recovery of creep-produced structures since dislocation pile-ups are rarely observed after creep [9–11].

Hausselt and Blum [12] considered that recovery during creep may be dynamic in nature; that is, the recovery process is affected by simultaneous dislocation creep processes. Evidence in support of their suggestion has been obtained from the general shape of the dislocation recovery plots and, in particular, the stress and dislocation density dependencies of recovery.

The influence of intragranular particles on dislocation recovery has been examined by several authors [2, 5, 13]; in general, the particles are considered to impose a friction stress inhibiting recovery, according to [13].

$$\frac{dl}{dt} = M \frac{\tau}{l} (1 - Zl)^2 \quad (3)$$

where M is the mobility term from Equations 1 or 2, corresponding to the particular operative diffusional mechanism; τZ is the frictional force on the dislocation links with Z being related to the reciprocal of the particle spacing. More recently, Engberg [5] has proposed that each dislocation link is completely free to recover until it meets a particle, at which point it becomes completely immobile. The influence of particles on recovery is thus expected to be critically dependent on the relative magnitudes of dislocation link lengths and interparticle spacings and on the distribution of dislocation link lengths.

*Now at Institute Cerac S.A., Ecublens, Switzerland.

0022–2461/79/112625–12 $03.20/0

TABLE I Analysis (wt %) of Type 316 steel

C	Si	Mn	Cr	Ni	Mo	S	P	B
0.057	0.70	1.08	16.86	11.32	2.09	0.009	0.028	0.0003

Dislocation recovery in a creep strained material reduces the flow stress such that yielding occurs on reloading at a stress lower than the original flow stress [2, 3]. Similarly, re-imposition of the original stress leads to a period of rapid strain before the original, steady strain rate is achieved [12]. Both the decrease in flow stress [2, 3] and the transient creep strain [12] correlate well with the observed decreases in dislocation density.

The present work attempts to elucidate the mechanism of dislocation recovery in a Type 316 austenitic stainless steel after creep straining and to examine the role of the intragranular carbides precipitated during the creep test in the recovery process. An improvement in the knowledge of such processes will undoubtedly lead to a better understanding of the mechanism of creep [14, 15, 16]; furthermore, since dislocation recovery occurs during stress relaxation [12, 17], it is to be expected that the extent of stress relaxation is affected by such recovery. Finally, the dislocation recovery and associated reloading effects have been studied so as to relate such reloading effects to similar loading transients observed during cyclic creep testing [18].

2. Experimental procedure

The analysis of the medium carbon Type 316 austenitic steel used in the present investigation is given in Table I. Round cross-section creep specimens were machined from hot-rolled bars of the steel, solution treated in argon at 1050° C for 0.75 h and finally quenched into water to produce a mean grain size of 50×10^{-6} m.

The creep tests were carried out in air at constant load, mainly at 625° C but with some testing at 700 and 550° C, using Dennison lever machines; the tests were terminated in the steady state creep stage by lowering the creep furnace and rapidly cooling the specimens under load in a stream of cold air. The creep deformations at the relevant stresses and temperatures have been detailed previously [9, 19]. The recovery anneals were usually conducted in air on sections of the gauge lengths of the creep strained specimens. However, some recovery anneals were performed under stress in the creep machines and the specimen finally rapidly cooled as above. The effects of dislocation recovery on the reloading behaviour were examined *in situ* by ageing specimens without stress in the creep furnaces prior to reloading. Each specimen was retested several times in this way; the loading strain was measured and the creep rate allowed to achieve a steady value on each occasion.

Thin foils were prepared from the gauge lengths of the creep strained and creep strained and recovered specimens and examined by transmission

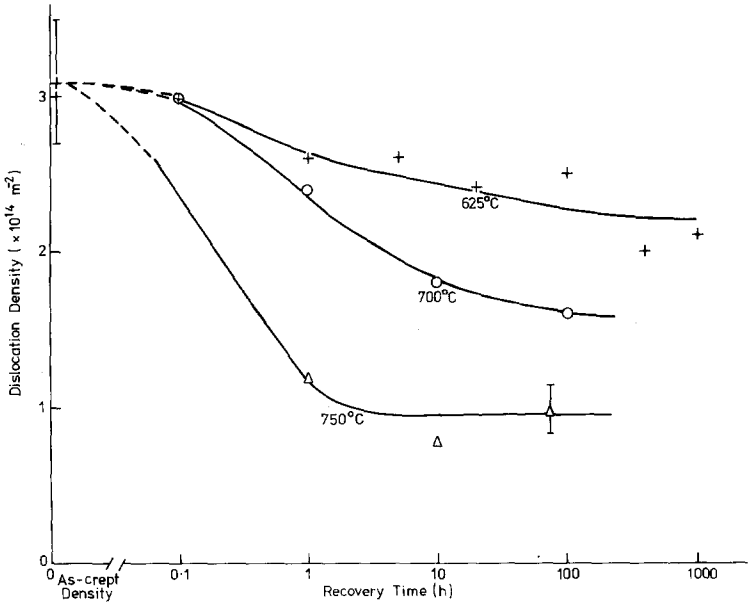

Figure 1 The variation of dislocation density with recovery time and temperature. Specimens initially creep-strained at 625° C and 200 MPa to the secondary creep stage.

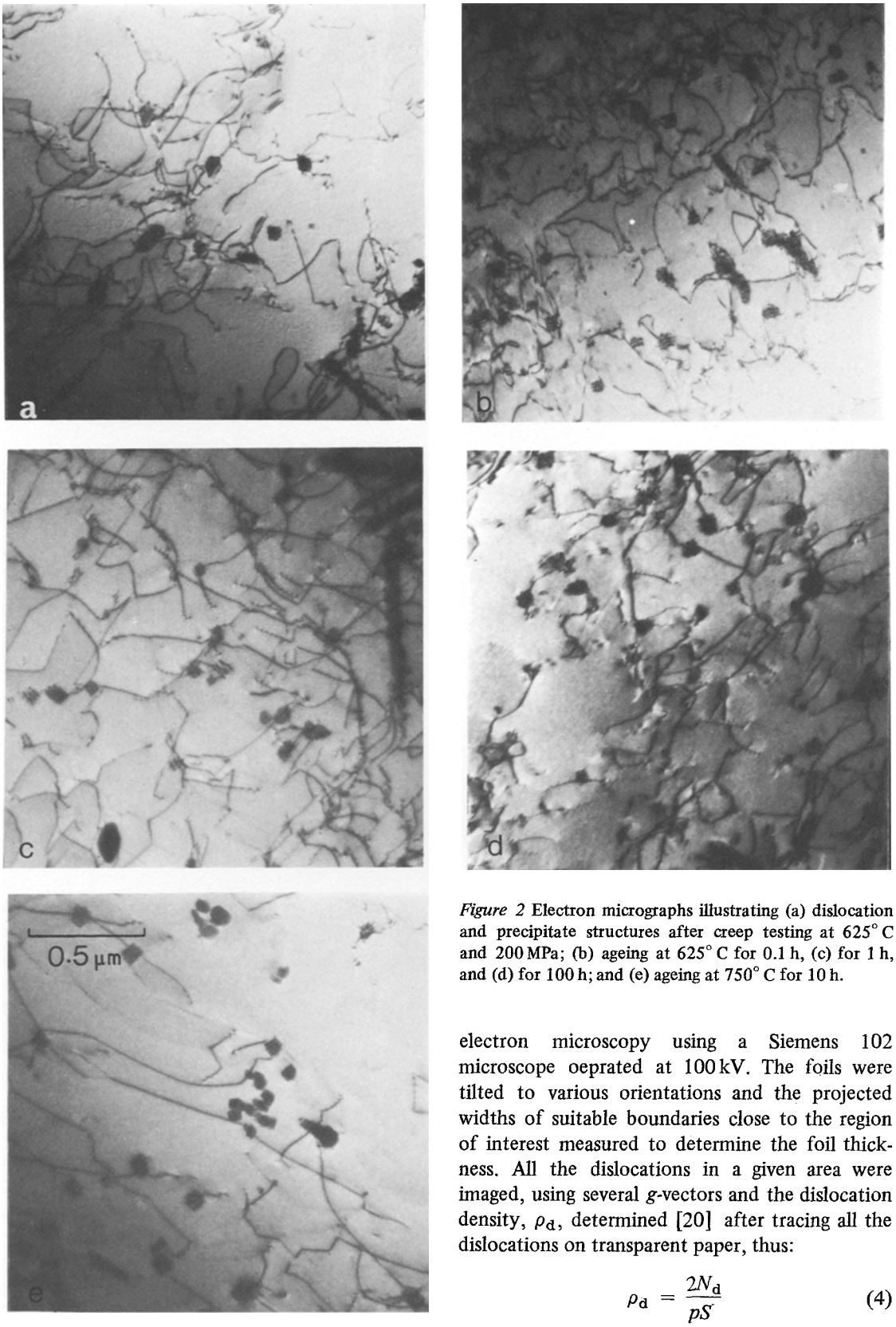

Figure 2 Electron micrographs illustrating (a) dislocation and precipitate structures after creep testing at 625° C and 200 MPa; (b) ageing at 625° C for 0.1 h, (c) for 1 h, and (d) for 100 h; and (e) ageing at 750° C for 10 h.

electron microscopy using a Siemens 102 microscope oeprated at 100 kV. The foils were tilted to various orientations and the projected widths of suitable boundaries close to the region of interest measured to determine the foil thickness. All the dislocations in a given area were imaged, using several g-vectors and the dislocation density, ρ_d, determined [20] after tracing all the dislocations on transparent paper, thus:

$$\rho_d = \frac{2N_d}{pS} \tag{4}$$

At least five areas were examined and more than 500 dislocation intersections considered for each specimen and condition; the errors in dislocation density were estimated from the spread in batches of data to be ±10 to 15%. The carbide particle density and size were also measured for each specimen [9]. The distribution of dislocation link lengths was ascertained in representative specimens using techniques described previously [4, 9, 21, 22].

3. Results

Fig. 1 shows the influence of recovery anneals of between 0.1 and 1000 hours duration at 625, 700 and 750° C on the dislocation densities of specimens tested at 625° C and an initial stress of 200 MPa to the steady state creep stage; typical error bars are illustrated for two of the data points only. The dislocation densities decrease significantly during the first ten hours or so of annealing but thereafter tend to remain sensibly constant; the magnitudes of the reductions in dislocation density increase with increasing temperature.

Typical electron micrographs of the dislocation and precipitate structures in the creep strained and strained and recovered specimens are shown in Fig. 2. The dislocation and intragranular carbide densities are presented as a function of recovery time at 625° C and initial creep stress and test temperature in Fig. 3 and Table II. The carbide densities are only marginally affected by the recovery treatments applied. However, the dislocation and carbide densities increase with increasing creep stress (and possibly decreasing temperature) for the specimens initially creep tested isothermally at 625° C and 700° C. In the case of the specimen tested initially at 625° C, 200 MPa and then at 550° C, 350 MPa for 10 h, the carbide density remains at the value determined by the creep test at 625° C, 200 MPa; furthermore, the initially high dislocation density in this specimen decreases rapidly with increasing recovery time up to 100 hours at 625° C to a value commensurate with the carbide density. The inhibition of dislocation recovery by a high density of intragranular particles is also evident when comparing the data for the specimen

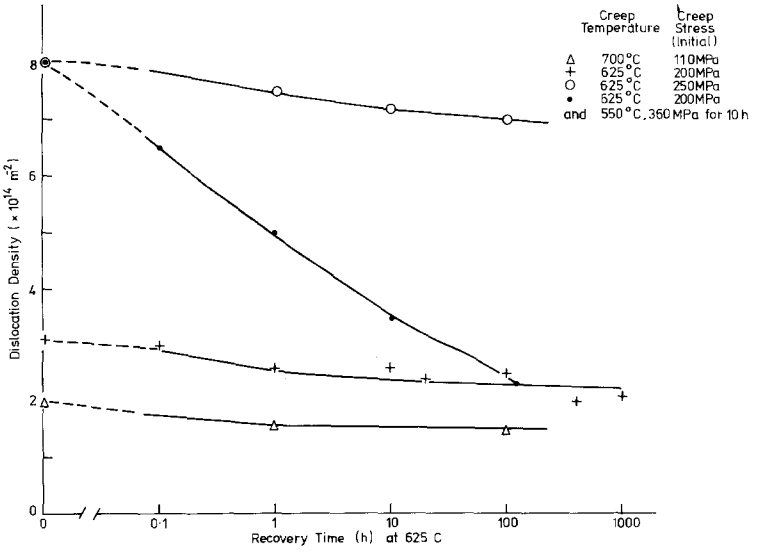

Figure 3 The variation of dislocation density with recovery time at 625° C for various initial creep testing conditions.

TABLE II Intragranular carbide and dislocation densities after recovery for 100 hours at 625° C for a range of initial creep structures

Creep stress (initial) (MPa)	Creep temperature (° C)	Intrangranular carbide density ($\times 10^{19}$ m^{-3})	Dislocation density after recovery ($\times 10^{14}$ m^{-2})
119	700	8	1.5
200	625	12	2.2
250	625	50	7
(200 MPa and 625° C followed by 360 MPa and 550° C for 10 h)		12	2.2

creep strained at 625° C, 200 MPa and the sample tested at 625° C, 200 MPa and 550°, 360 MPa. The temperature dependence of the recovery in the latter, high dislocation density–low carbide density material is illustrated in Fig. 4; there is a rapid reduction in dislocation density during the initial stages of annealing but the rate of recovery decreases at the longer times when low dislocation densities have been achieved.

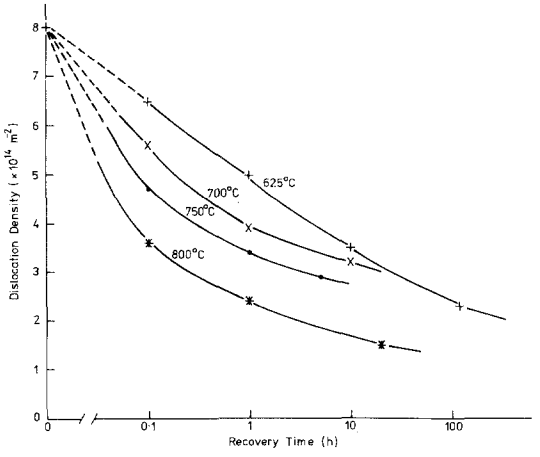

Figure 4 The time and temperature dependencies of the recovey of dislocation density in specimens creep-strained initially at 625° C, 200 MPa and then at 550° C, 360 MPa for 10 hours.

The effects of the intragranular particles on the saturation dislocation density observed after recovery were examined by loading a series of specimens at 625° C to increasing strains and then ageing for 300 h at the same temperature. The results are given in Table III and the mean intragranular carbide spacing, λ_c, is plotted against the mean dislocation link length, $\bar{l}$, in Fig. 5. The two parameters are linearly related, thus:

$$\frac{\lambda_c}{\bar{l}} = 3 \qquad (5)$$

thereby providing additional evidence for stabilization of the dislocation density by the intergranular carbide precipitates.

The dislocation link lengths produced during creep follow a Gaussian type distribution with the median and maximum dislocation link lengths corresponding to about $\lambda_c/3$ and λ_c respectively [9]; this is confirmed by the results of the present work shown in Fig. 6. The distribution of link lengths changes during recovery as the fraction of very short link lengths decreases and the fraction

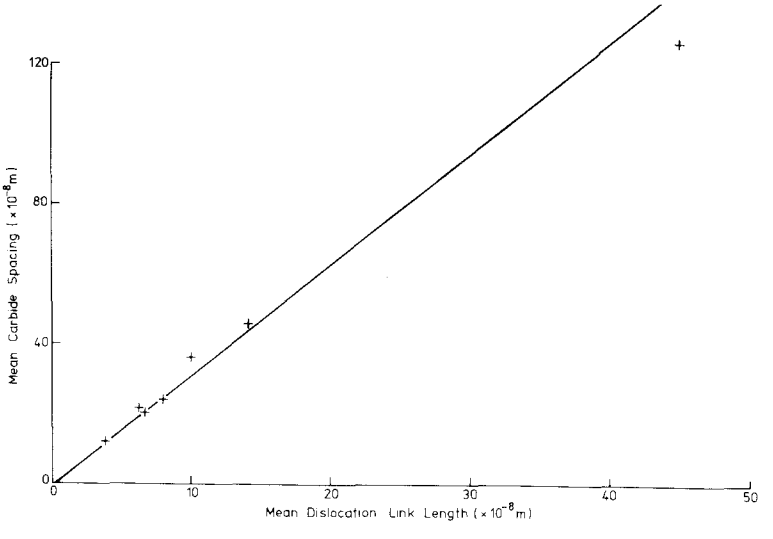

Figure 5 The variation of mean intragranular carbide spacing with the mean dislocation link length after recovery.

TABLE III Intragranular carbide density and spacing and dislocation density and mean link length after straining and ageing for 300 hours at 625° C

Strain (%)	Carbide density ($\times 10^{19}$ m^{-2})	Mean carbide spacing ($\times 10^{-8}$ m)	Dislocation density (m^{-2})	Mean dislocation link length ($\times 10^{-8}$ m)
0	0.05	125	5×10^{12}	45
4	1	46	5×10^{13}	14.1
6	2	36.8	10^{14}	10
9	8	23.2	1.5×10^{14}	8.2
12	10	21.5	2.5×10^{14}	6.3

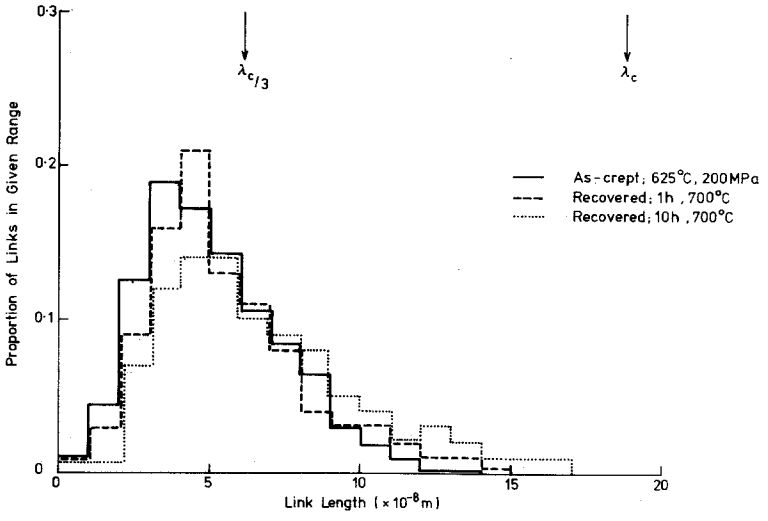

Figure 6 Dislocation link length distributions observed after creep straining and after partial recovery.

of large links increases; the mean dislocation link length increases slowly as the dislocation density decreases.

Particle coarsening occurs throughout the recovery anneals but the rate of coarsening at the recovery temperatures investigated is slow. It is not possible to examine the coarsening process in detail from the data obtained and high recovery temperatures were not used because the increased carbon solubility leads to carbide dissolution. Nevertheless, despite the inaccuracies in the present data, it appears that the coarsening can be described (see Fig. 7) thus [23, 24]:

$$r_t^3 - r_0^3 = \frac{8DB\gamma}{9kT}\Omega t \qquad (6)$$

The activation energy determined for the process, $\sim 260\,\mathrm{kJ\,mol^{-1}}$, should correspond to the sum of the activation energies for diffusion and for solution [23, 24]. The activation energy for self-diffusion is approximately 280 kJ mol [25] and that for a solution of $M_{23}C_6$ may be estimated as 50 to 100 kJ mol [26]. The sum of the values is much larger than the experimentally determined value, suggesting that pipe diffusion (for which the activation energy is approximately 0.6 that for self-diffusion [27]) plays an important part in the coarsening. However, uncertainties in the experimental determinatons and the value of the activation energy of solution do not warrant any further analysis of the coarsening mechanisms here.

Since the results presented above show little influence of the intra-granular particles on recovery when the dislocation density is very high, the effects of stress applied during the recovery anneal was studied on specimens initially creep strained at 625° C, 200 MPa to the secondary creep stage and then at 550° C, 360 MPa for 10 h. The

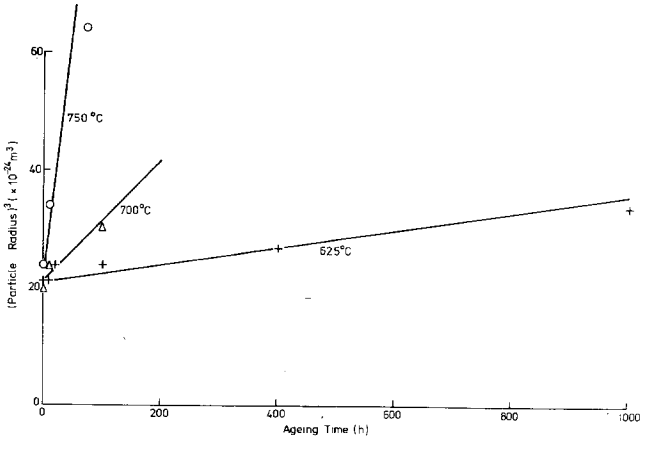

Figure 7 Particle coarsening during recovery.

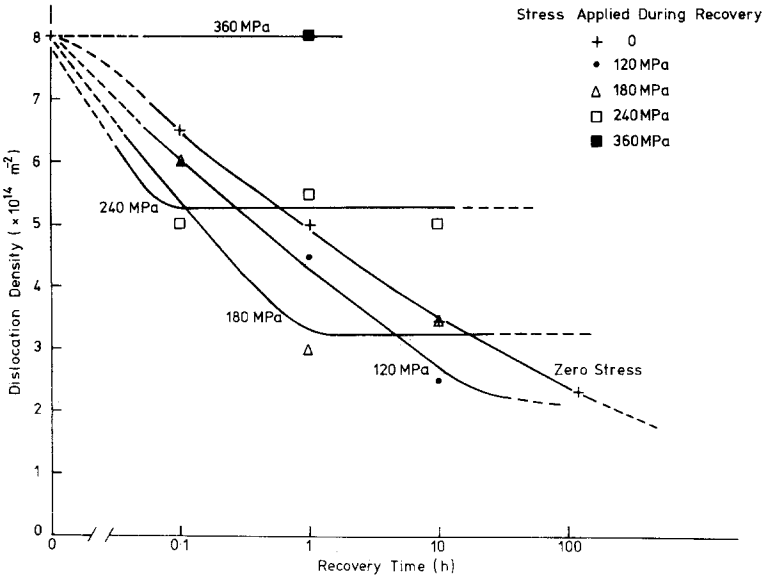

Figure 8 The influence of stress on the rate of recovery and saturation dislocation density. Specimens initially creep strained at 625° C, 200 MPa^{-1} and then 550° C, 360 MPa^{-1} for 10 h.

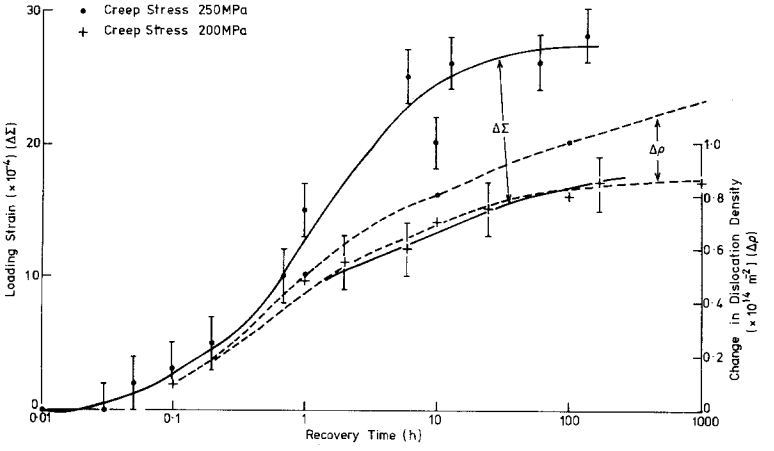

Figure 9 The effect of recovery on the reloading strains and the change in dislocation density during recovery for two initial creep stress conditions at 625° C.

recovery characteristics at 625° C for various applied stresses are shown in Fig. 8. The rate of dislocation recovery is accelerated by the applied stress and the dislocation density saturates at progressively higher values with increasing stress. A stress of 360 MPa produces, as expected, no change in the dislocation density.

The effect of dislocation recovery in the absence of stress on the subsequent loading strains is illustrated in Fig. 9 for specimens initially creep strained at 625° C, 200 and 250 MPa. The reductions in dislocation density during recovery, as deduced, for example, from Fig. 1, are also included in Fig. 9. The changes in dislocation density ($\Delta\rho$) and loading strain ($\Delta\Sigma$), obtained using the same reloading and initial creep stresses, are linearly related as follows:

$$\Delta\rho \simeq 3 - 5 \times 10^{16} \Delta\Sigma \qquad (7)$$

expressing $\Delta\rho$ as lines m^{-2} and $\Delta\Sigma$ as true strain.

4. Discussion

The rate of dislocation recovery according to the jog climb mechanisms (Equations 1 and 2) may be expressed, using $\bar{l} = \rho^{-1/2}$, as:

$$\frac{1}{\rho_t} - \frac{1}{\rho_0} = Kt \qquad (8)$$

The present recovery data (Figs. 1, 3 and 4) show that this expression does not describe recovery for any of the conditions examined and that the initial rapid recovery rates are always followed by very

much slower recovery rates which are associated with precipitation effects.

The recovery data may be analysed using Equation 3, derived by Lagneborg [13] to account for the friction stress imposed on dislocation links, with $Z = \sigma_0/\alpha\mu b$ [13], σ_0 may be expressed [28] as $\sigma_0 = 2\mu b \cos(\phi/2)/\lambda_c$, where ϕ is a very large ($\sim 150°$) for the $M_{23}C_6$ particles produced in the Type 316 steel [29]. Equation 3 may now be written as:

$$\frac{1}{\rho^2}\frac{d\rho}{dt} = -M\tau\left[1 - \frac{\rho^{-1/2}}{A\lambda_c}\right]^2 \quad (9)$$

where $A = 1/[2\cos(\phi/2)] = \sim 4$.

Fig. 10 shows a plot of $(1/\rho^2)(d\rho/dt)$ against $[1-(\rho^{-1/2}/A\lambda_c)]^2$ for several values of A. A straight line passing through the origin is expected if the Lagneborg model of recovery inhibition applies; it is obvious from Fig. 10 that the recovery data cannot be described in terms of this model and hence it is concluded that particles do not inhibit recovery by exerting a general friction stress on the dislocations. As described by Engberg [5], it appears that the particles are more likely to inhibit significantly the climb recovery of dislocation links only when the particles intersect the links. Thus, short dislocation links are capable of climbing quickly, leading to an initially high recovery rate, whilst longer dislocations are almost completely immobile. This interpretation is consistent with the observed rapid disappearance of the short dislocation link lengths during recovery anneals (Fig. 6) and also with the electron metallographic evidence (Fig. 2). There are many short links unpinned by particles in the "as-creep strained" specimen whilst an increasing proportion of the dislocation links lie on particles after long recovery times. At the prolonged recovery times the rate of dislocation recovery is determined by the rate of precipitate coarsening [30], the rate of recovery by dislocation unpinning from the particles being very low.

The data and observations on the early stages of recovery have been used to analyse essentially free dislocation recovery behaviour in the instances where particle [5] or solute [4, 31] inhibition of dislocation recovery is observed after long recovery times. The data for the specimens initally creep-strained at 625° C and then at 550° C can be used for such an analysis in the present work. Equation 8 may be differentiated as:

$$\frac{d\rho}{dt} = -K\rho^2 \quad (10)$$

The values of K obtained from an analysis of the recovery data in Fig. 4 are shown for several dislocation densities in Fig. 11; these data yield a mean activation energy of $260 \pm 40\,\text{kJ mol}^{-1}$. This value is close to the activation energy for bulk diffusion [25] suggesting that the jogs on the climbing dislocations are fully saturated with vacancies [6]; consequently, Equation 2 is expected to describe the coarsening process. With $l = \rho^{-1/2}$, Equations 1 and 2 can be written as:

$$\frac{1}{\rho^2}\frac{d\rho}{dt} = -\frac{4D_s b}{kT}\tau \times E \quad (11)$$

where E is C_j (Equation 1) or $1/[\ln(l/b)]$ (Equation 2) and the right hand side of Equation 11 may be equated with K in Equation 10.

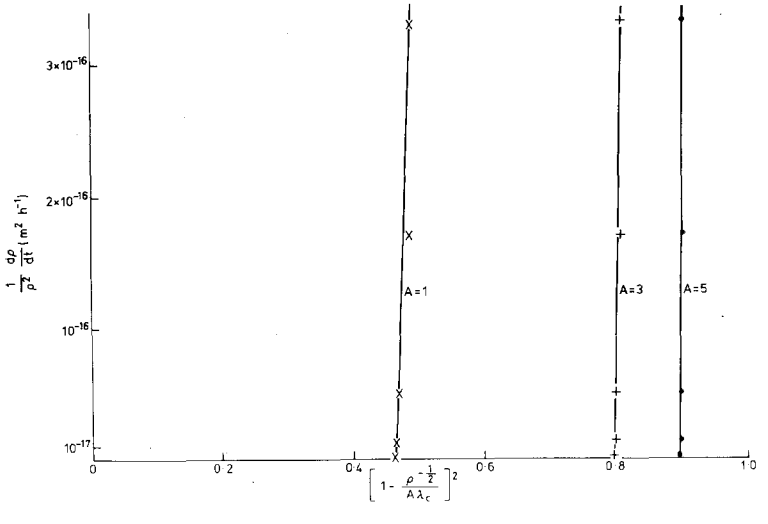

Figure 10 A plot of $(1/\rho^2)(d\rho/dt)$ against $[1-(\rho^{-1/2}/A\lambda_c)]^2$ for specimens creep strained initially at 625° C, 200 MPa and subsequently recovered at 625° C.

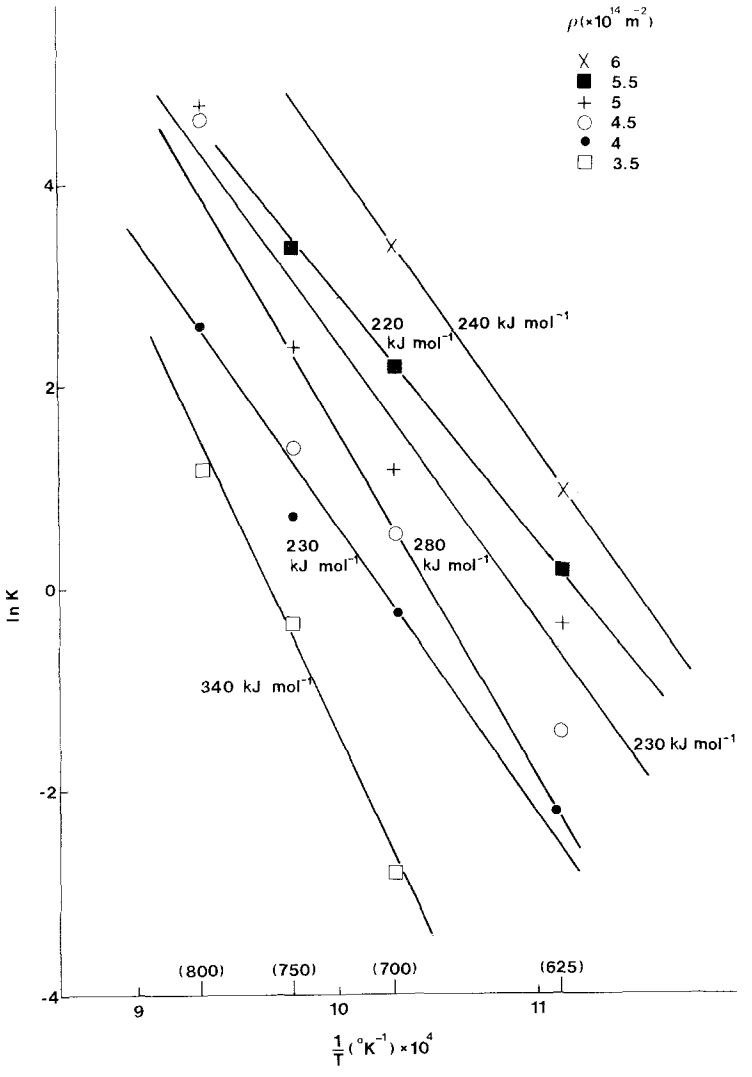

Figure 11 The activation energies for dislocation recovery determined from the rate of recovery $[(1/\rho^2)(d\rho/dt)]$ at given values of dislocation density.

From the values of K given in Fig. 11, E is estimated to be 0.5, independent of temperature. If the jogs on dislocations are fully saturated with the vacancies, then $E\,(=1/[\ln(l/b)])\simeq 0.2$, in reasonable agreement with the experimentally deduced value.

The recovery rate is proportional to the square of the dislocation density according to the network coarsening model (Equation 10). The observation that the recovery rate is not dependent on the square of the dislocation density was used by Hausselt and Blum [12] as evidence for dynamic recovery with dislocation glide also playing a part in the recovery process. The dislocation density dependencies of the recovery rate at 625° C are shown in Fig. 12 for specimens creep tested at 625 and 625 to 550° C; these data indicate that the recovery rates are dependent on the dislocation densities to the power 28 and 7 respectively. Since these situations correspond to severely inhibited and slightly inhibited recovery respectively, it is evident that the precipitated particles are responsible, at least in the present work, for the deviations in behaviour from simple theory. The increasing influence of a given density of particles in inhibiting dislocation motion as the dislocation density decreases has been demonstrated in Fig. 3.

Blum [32, 33, 12] has shown that the creep rate ($\dot{\Sigma}$) may be predicted from the dislocation recovery rate $\bar{\dot{\rho}}$, thus:

$$\dot{\Sigma} = \frac{b}{F} L \bar{\dot{\rho}} \qquad (12)$$

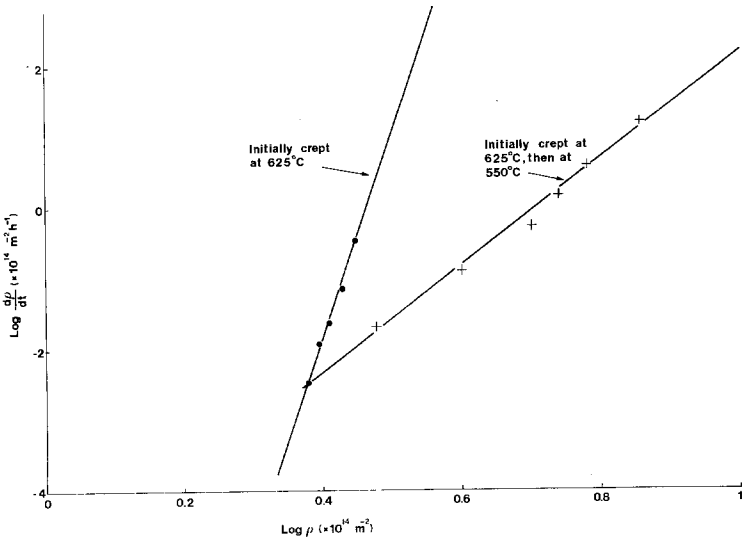

Figure 12 The dislocation recovery rate at 625° C as a function of dislocation density for specimens initially creep strained at 625° C, 200 MPa with and without subsequent straining at 550° C, 360 MPa^{-1} for 10 h.

Using a value of the dislocation recovery rate for the "as-creep strained" specimen derived from Fig. 12 and taking $L \simeq \bar{l} = \rho^{-1/2}$, a creep rate of 1×10^{-7} sec^{-1} is calculated; this compares with an experimentally determined value of 6×10^{-8} sec^{-1} [9]. This small discrepancy is undoubtedly due to the use of an incorrect value of L, since the mean dislocation slip distance is probably less than mean spacing of dislocations. The stress dependence of the creep rate may be predicted from Equation 12 with, again, $L \simeq l = \rho^{-1/2}$ and $\sigma = \mu b \rho^{+1/2}$. The stress dependencies of L and $\bar{\rho}$ are -1 and 14 respectively for specimens creep tested at 625° C, 200 MPa; this indicates a stress dependence of the creep rate of 13 compared with an experimentally determined value of 12 [9]. The present data therefore provide further support for the conclusion that the stress dependence of the creep rate in precipitation hardened materials is determined by the effect of the precipitate particles on the dislocation recovery rate [9].

The application of stress during climb leads to a greater energy reduction as dislocation link straightening and network coarsening occurs. Nordstrom and Barrett [3] calculated that the recovery rate is increased by a factor of two by the application of the creep stress during the recovery. The present results (Fig. 8), whilst insufficiently accurate to merit detailed analysis, support this conclusion. The increased saturation level of dislocation density as the stress increases is a reflection of the extent of creep, and network refining, that occurs when significant stresses are imposed.

The loading strains produced on applying a stress of 250 MPa after recovery unstressed (Fig. 9) are consistent with the strains observed previously during cyclic creep testing [18] and confirm that no cyclic-produced change in structure occurs in such tests. The incremental strains and dislocation density changes during recovery are linearly related, a feature that may be analysed as follows. The stress–strain curve for stainless steels may be approximated by:

$$\sigma = \sigma_y + J\Sigma_p^{1/2} \tag{13}$$

where σ is the stress corresponding to a plastic strain Σ_p. The work hardening component of stress, $J\Sigma_p^{1/2}$, may be related to the dislocation density as $\mu b \rho^{1/2}$. In the context of the incremental dislocation recovery and strain effects, these terms can be equated as:

$$\mu b(\Delta\rho)^{1/2} = J(\Delta\Sigma)^{1/2} \tag{14}$$

giving

$$\Delta\rho = \left(\frac{J}{\mu b}\right)^2 \Delta\Sigma \tag{15}$$

The proportional factor in Equation 15 was evaluated from the results of tensile tests carried out at an initial strain rate of 5% min^{-1} at 625° C as 4×10^{15}, a factor of 10 smaller than the experimentally deduced value of 3 to 5×10^{16} (Equation 8). The discrepancy in strain increments produced by given dislocation density increments probably arises from the different distribution of link lengths associated with the deformed and the recovered states (Fig. 6). Thus, conventional tensile straining

involves increasing the density of dislocation links of all lengths, whilst the smaller strain increments observed on reloading after recovery result primarily from increases in the density of very short dislocation links.

5. Conclusions

(1) The rate of recovery of dislocation density during the annealing of creep strained Type 316 stainless steel is initially rapid but subsequently decreases as a saturation dislocation density is approached.

(2) The level of the saturation dislocation density is related to the intragranular precipitate density produced during the prior creep straining by $\rho^{-1/2} = \bar{l} = \lambda_c/3$.

(3) The influence of particles in inhibiting recovery is not associated with a general friction stress as suggested by Lagneborg: the data are more consistent with Engberg's proposal that the dislocation links can move if no precipitates intersect the links but are completely immobilized when intersected by particles.

(4) Analysis of the early stages of recovery, when the precipitate inhibiting effect is small, suggests that dislocation recovery occurs by dislocation climb, the rate controlling process being vacancy diffusion between the dislocation links.

(5) Application of stress during recovery leads to an enhancement of the recovery rate in accordance with the Friedel model of network growth.

(6) The incremental strains produced on reloading after recovery can be correlated with the reductions in dislocation density induced during the recovery period.

Appendix 1

List of symbols and appropriate values

l	dislocation link length
D_s	self diffusion coefficient
b	Burgers vector (2.5×10^{-1} m)
C_j	equilibrium jog concentration
τ	dislocation link tension
k	Boltzman's constant (1.38×10^{-23} J atom^{-1} K^{-1})
T	absolute temperature
t	recovery time
M	mobility term
Z	frictional term associated with particles
ρ_d	dislocation density determined from micrographs
N_d	number of dislocation intersections on test line
p	length of test line
S	foil thickness
$\bar{l}$	mean dislocation link length
λ_c	mean intragranular particle (carbide) spacing
r_0	mean intragranular particle radius at time $t = 0$
r_t	mean intragranular particle radius at time t
D	solute diffusion coefficient
B	solubility of $M_{23}C_6$ in austenite
γ	particle–matrix interface energy
Ω	atomic volume (10^{-29} m^3)
$\Delta\rho$	change in dislocation density during recovery period
$\Delta\Sigma$	incremental strain associated with reloading after recovery period
K	constant
ρ	dislocation density
ρ_0	dislocation density at time $t = 0$
ρ_t	dislocation density at time t
σ_0	friction stress associated with particles
α	constant ($\simeq 1$)
μ	shear modulus
ϕ	angle between dislocation segments as dislocation breaks through a particle
A	$1 \cos(\phi/2)$
E	constant
$\dot{\Sigma}$	creep rate
F	Taylor factor
L	mean slip distance of dislocations
$\dot{\bar{\rho}}$	rate of dislocation recovery
σ	stress
σ_y	yield stress
J	strength coefficient
Σ_p	plastic strain

References

1. R. W. CAHN, in "Physical Metallurgy," edited by R. W. Cahn (North-Holland, London, 1970) p. 1129.
2. T. V. NORDSTROM and C. R. BARRETT, *J. Mater. Sci.* 7 (1972) 1037.
3. T. V. NORDSTROM and C. R. BARRETT, *J. Mater. Sci.* 7 (1972) 1052.
4. A. ODEN, E. LIND and R. LAGNEBORG, Proceedings of the I.S.I. Conference on "Creep Strength in Steels and High Temperature Alloys", Sheffield, 1972 (The Metals Society, London 1974).
5. G. ENGBERG, TRITA-MAC-00098, Royal Inst. Technology, Stockholm, October 1976.

6. J. FRIEDEL "Dislocations" (Pergamon Press, Oxford, 1964).
7. F. R. N. NABARRO, *Phil. Mag.* **16** (1967) 231.
8. J. WEERTMAN, *J. Appl. Phys.* **28** (1957) 362.
9. D. G. MORRIS, *Acta Met.* **26** (1978) 1143.
10. R. LAGNEBORG, *Int. Met. Rev.* **17** (1972) 130.
11. K. D. CHALLENGER and J. MOTEFF, *Met. Trans.* 4 (1972) 749.
12. J. HAUSSELT and W. BLUM, *Acta Met.* **24** (1976) 1027.
13. R. LAGNEBORG, *J. Mater. Sci.* **3** (1968) 596.
14. R. W. BAILEY, *J. Inst. Metals* **35** (1926) 27.
15. E. OROWAN, *J. West Scotland I.S.I.* **54** (1946-47) 45.
16. D. McLEAN, *Reports Prog. Phys.*, **29** (1966) 1.
17. W. L. BRADLEY, W. RENFROE and D. K. MATLOCK, *Scripta Met.* **10** (1976) 905.
18. D. G. MORRIS and D. R. HARRIES, *J. Mater. Sci.* **13** (1978) 985.
19. D. G. MORRIS and D. R. HARRIES, *Metal Sci.* **12** (1978) 525.
20. P. B. HIRSCH, A. HOWIE, R. B. NICHOLSON, D. W. PASHLEY and M. J. WHELAN, "Electron Microscopy of Thin Crystals" (Butterworths, London, 1965).
21. R. LAGNEBORG, B. H. FORSEN and J. WIBERG, Proceedings of the I.S.I. Conference on "Creep Strength in Steels and High Temperature Alloys", Sheffield, 1972 (The Metals Society, London, 1974).
22. B. MODEAR and R. LAGNEBORG, *Jernkont Ann.* **155** (1971) 363.
23. C. WAGNER, *Z. Electrochem* **65** (1961) 581.
24. I. M. LIFSHITZ and U. U. SLYOSOV, *J. Phys. Chem. Solids,* **19** (1961) 35.
25. H. J. FROST and M. F. ASHBY, "Deformation-Mechanism Maps for Pure Iron Two Austenitic Steels and a Low Alloy Ferritic Steel", Cambridge University, Eng. Dept. Report, September, (1975).
26. "Metals Reference Book", edited by C. J. Smithells (Butterworths, London, 1976).
27. R. W. BALLUFFI, Cornell University Materials Science Centre Report NYO-3504-42, March (1970).
28. A. J. E. FOREMAN and M. J. MAKIN, *Phil. Mag.* **14** (1966) 911.
29. D. G. MORRIS, *J. Mater. Sci.* **13** (1978) 1849.
30. R. J. McELROY, Y. ISHIDA, D. McLEAN and Z. SZKOPIAK, *Metals Tech.* **1** (1974) 468.
31. J. P. HIRTH and J. LOTHE, "Theory of Dislocations", (McGraw-Hill, New York, 1968).
32. W. BLUM, *Phys. Stat. Sol. (b)* **45** (1971) 561.
33. W. BLUM, *Z. Metallkunde* **63** (1972) 757.

Received 14 February and accepted 28 March 1979.